journal

J. Am. Ceram. Soc., **85** [6] 1414–20 (2002)

Preparation of Strontium- and Zinc-Doped $LaGaO_3$ Powders via Precipitation in the Presence of Urea and/or Enzyme Urease

A. Cüneyt Taş,*,† Peter J. Majewski, and Fritz Aldinger*

Max-Planck-Institut fuer Metallforschung, Pulvermetallurgisches Laboratorium, Stuttgart D-70569, Germany

Solid oxide fuel cell powders having a composition of $La_{0.8}Sr_{0.2}Ga_{0.8}Zn_{0.2}O_{2.8}$ (LSGZ) were prepared by aqueous chemical precipitation in the presence of decomposing urea, followed by single-step calcination in air. In some synthesis experiments the decomposition of urea was catalyzed by the enzyme urease. The calcination behavior of the precursor powders was studied over the temperature range of 90–1300°C, in an air atmosphere. Characterization of the samples was performed by XRD, TG/DTA, FTIR, FESEM, EDS, and carbon analyses. Two tentative XRD patterns have been created for the hydroxycarbonate precursors and the product LSGZ ceramics, respectively.

I. Introduction

THE growing interest during the last decade in solid oxide fuel cells (SOFCs) has mainly been the progression of the long-time quest of developing more efficient power generation devices.[1] Sr- and Mg-doped $LaGaO_3$ (LSGM) distorted-perovskite ceramics were recently discovered[2,3] to have superior oxygen ion conducting properties as compared with yttria-stabilized zirconia electrolytes. Promising ionic conduction performance[4–6] and the mechanical properties[7–11] of LSGM ceramics have already been reported. Sr- and Mg-doped $LaGaO_3$ ceramics were typically synthesized by the conventional solid-state reactive firing (i.e., mixed oxide) method.[2–13] Stevenson *et al.*[14,15] have used the technique of combustion synthesis[16,17] in preparing Sr- and Mg-doped $LaGaO_3$ powders, and more recently, combustion synthesis of LSGM ceramics has been reported for the manufacture of thin films of the same.[18] Djurado *et al.*[19] and Maric *et al.*[20] studied the technique of spray pyrolysis for the manufacture of submicrometer LSGM powders. The characteristic of oxygen permeation through composites consisting of LSGM ceramics and noble metals (such as Pd or Ag) was also reported.[21] The influence of various transition-metal dopants, such as Co,[22–28] Fe,[26,27,29] Mn,[26,29] Cr,[26,27] V,[26] Cu, Ni, and Zn[29] on the conductivity of such ceramics (all prepared by using the conventional mixed-oxide route) has also been examined.

On the other hand, wet chemical syntheses of this family of solid electrolyte compounds have received relatively little attention. The route of coprecipitation (with NH_4OH addition), starting with an aqueous mixture of the acetates of La, Sr, and Mg, and of gallium nitrate, have been studied for the first time by Huang *et al.*[30] Huang *et al.*, in a separate paper,[31] have also briefly mentioned the use of Pechini method[32–34] for the synthesis of LSGM powders. In a previous study, we also have tested the Pechini method for preparing fine powders of LSGM stoichiometry, following the high-temperature calcination of the obtained Pechini resins.[35]

Synthesis of inorganic powders by aqueous precipitation in the presence of decomposing urea (CH_4N_2O) is not an original concept of this study, and this method has previously been shown to work satisfactorily in different material systems by Matijevic,[36–38] and others.[39–43] Synthesis of ceramics by enzyme-catalyzed reactions, which are performed in aqueous solutions, have also been studied by Gauckler *et al.*[44]

In the present paper, a simple chemical preparation route is described, for the first time, for the preparation of Sr- and Zn-doped $LaGaO_3$ (LSGZ: $La_{0.8}Sr_{0.2}Ga_{0.8}Zn_{0.2}O_{2.8}$) ceramic powders in the presence of decomposing urea and/or enzyme urease.

II. Experimental Procedure

The powders were synthesized by using 0.15–0.75*M* separate stock solutions of each of the following chemicals: $La(NO_3)_3 \cdot 0.9H_2O$ (>99%, Merck, Darmstadt, Germany), $Ga(NO_3)_3 \cdot xH_2O$ (99.999%, Sigma-Aldrich Chemie GmbH, Steinheim, Germany), $Sr(NO_3)_2$ (>99%, Merck), and $Mg(NO_3)_2 \cdot 0.6H_2O$ (>99%, Merck). The stock solutions were prepared by dissolving appropriate amounts of the starting chemicals in boiled deionized water. The value of *x* given (assigned by the manufacturer) in the formula of gallium nitrate was experimentally found to be 4.06 (by ICP-AES analyses we performed on the stock solutions). Urea and and enzyme urease (5 units/mg) used were reagent-grade (>99%, Merck). The molar ratio of urea to total cations (and therefore, its influence on the phase purity of the calcined precursor powders) in the precipitation solutions was investigated over the range of 10 to 30. The aging time and aging temperature were kept constant at 1 h and 90°C, respectively, throughout the entire experiments. The total cation concentration in the solutions was also kept constant at 0.05*M*.

The optimum recipe for the preparation of LSGZ–hydroxycarbonate precursor powders can be described as follows: A total of 24 mL (0.002 mol of La^{3+} and Ga^{3+} each, and 0.0005 mol of Sr^{2+} and Zn^{2+} each) of cation stock solutions was first mixed in a 150 mL capacity glass beaker. Deionized water (76 mL) containing 9 g of previously dissolved urea (and/or 50 mg of enzyme urease) was then added to this beaker. The solution was mixed for 15 min at 22 ± 1°C. Hydroxypropylcellulose (99%, Sigma) was also used (20 mg) as a dispersing agent. The final solution was then heated to 90 ± 1°C on a hot plate in about 60 min. As an alternative to the precipitation experiments performed in a beaker on a hot plate, it was found that placing the same amount of solution (as above) in a 100 mL capacity glass bottle (with a screw cap) and then placing this bottle in a microprocessor-controlled oven at 90°C and keeping it there for 90 min would produce precursor powders with a perfectly identical chemical composition and morphology. The formed precipitates, after 1 h of aging at a constant solution temperature of 90°C, were finally separated from the mother liquor by centrifugal filtration (9000 rpm, 10 min), followed by washing three to four times with 2-propanol (99%, Merck). The washed

N. J. Dudney—contributing editor

Manuscript No. 188304. Received August 24, 2000; approved January 31, 2002.
*Member, American Ceramic Society.
†Present address: Merck Biomaterial GmbH, F129/218, Darmstadt D-64271, Germany.

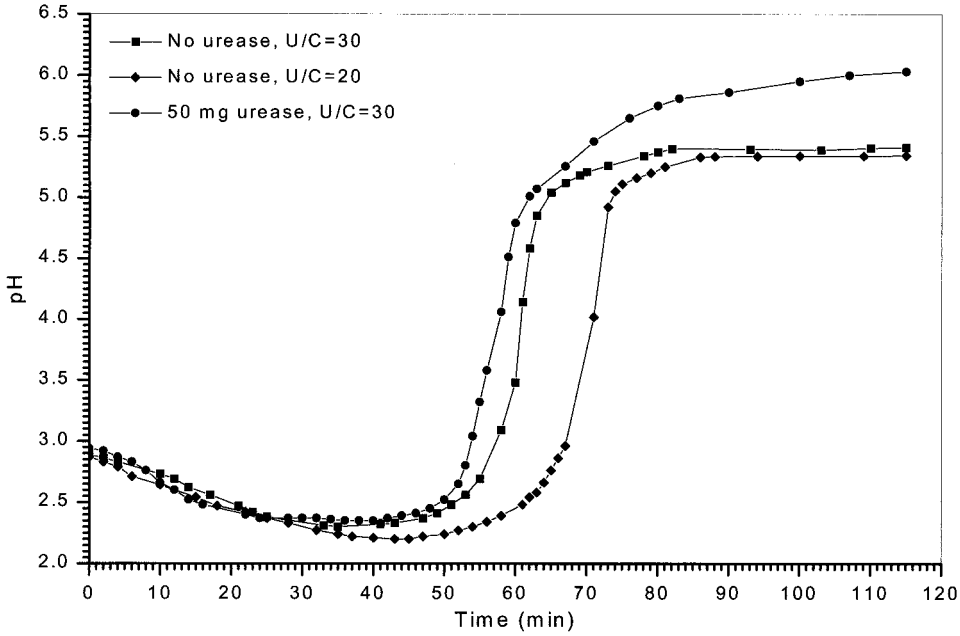

Fig. 1. Plots of pH versus time during LSGZ hydroxycarbonate precursor precipitation.

precipitates were oven dried at 90°C in air, overnight. Dried powders were finely ground by hand with an agate mortar/pestle, and then calcined, as loose powders, in alumina boats in air at various temperatures (350–1300°C). Each calcination batch was heated to the specified temperature at a rate of 5°C/min, soaked at this temperature for 6 h, and then cooled back to ambient at the same rate.

Phase distribution in the powders was analyzed as a function of calcination temperature by a powder X-ray diffractometer (D-5000, Siemens GmbH, Karlsruhe, Germany) and Cu$K\alpha$ radiation (40 kV, 30 mA, step size 0.016°, count time 1 s, 10–80° 2θ). A silicon external standard to correct for systematic errors was used, along with the Appleman Least Squares Refinement Program.[45]

Pyrolysis and decomposition of a 150 mg portion of the precursors were monitored by simultaneous differential thermal and thermogravimetric analysis (STA501, Bähr GmbH, Bremen, Germany) in air at a rate of 5°C/min. FTIR analyses of the samples were performed (IFS 66, Bruker GmbH, Karlsruhe, Germany) by mixing them (1 wt%) with dry KBr to form the pellets. The residual C contents of the uncalcined and calcined powders were determined by the combustion–IR absorption method (CS-800, Eltra GmbH, Neuss, Germany). The morphology and elemental constitution of the powders was studied by field-emission scanning electron microscopy (DSM 982 Gemini, Zeiss GmbH, Oberkochen, Germany) and EDS (6103, Oxford Microanalysis Group, Oxford, U.K.).

III. Results and Discussion

During homogeneous precipitation, the conditions of formation of a solid hydroxide or hydroxycarbonate phase in the synthesis beakers are governed by the controlled generation of hydroxide ions (as well as carbonate ions) through the decomposition of urea.[46] The presence of enzyme urease in solutions simply enhances the rate of decomposition of urea, especially at temperatures below 80°C.[44,47,48] The decomposition behavior of urea in aqueous solutions appears to depend on the urea concentration, as well as other variables such as temperature and the presence and amounts of cations in the solution.[49]

Decomposition of urea and the progress of precipitation in the La-, Sr-, Ga-, and Zn-containing solutions was followed in terms of pH changes, and a typical plot of pH versus reaction time is given in Fig. 1 for different solutions. In all of these, the solution temperature was raised from 22° to 90°C in about 60 min. It appeared that the initial drop in pH might be due to both the presence of acidic cations in the solution and, although not directly suggested by the data of Fig. 1, the formation of the intermediate complex HCNO,[50] followed by an increase in the ion product constant (K_w) of water, associated with a slow increase in temperature. The characteristic abrupt rise in pH seen in Fig. 1, for different urea-to-cation (U/C) ratios, coincided with the observation of a slight turbidity in the solution as precipitation started. Following this, a rather slow increase in pH was observed until the hydrolysis of cations was complete. On the completion of the decomposition of urea, the pH of the solution leveled off, and remained more or less the same during the rest of the aging period. The accurate sequence of chemical reactions describing the process of homogeneous decomposition of urea (at $T \geq 70$°C) was previously documented.[39,47] On the other hand, the influence of the U/C ratio and the presence of enzyme urease on the solution pH are also indicated by the data presented in Fig. 1. Enzyme urease, being a biological catalyst, would significantly increase the rate of urea decomposition at low ($T < 20$°C) solution temperatures, but it is not consumed by the process:[47] according to the reaction

$$NH_2\text{–}CO\text{–}NH_2 + 2H_2O + \text{urease} \rightarrow 2NH_4^+ + CO_3^{2-}$$

The reaction speed basically depends on temperature and the amount of enzyme urease added. One unit of urease, for instance, will liberate 1 μmol of NH_3 from urea per min at pH 7 and 25°C.[47,51] It was observed that the enzyme urease could be used to slightly increase the final pH value of the LSGZ–hydroxycarbonate precipitation solutions, as well as to decrease the incubation time for the formation of precipitates in the solutions. When the U/C ratio was kept below 20 (such as 10), it was not possible to obtain single-phase LSGZ, following the calcination of precursors at 1300°C for 6 h. In such cases, the observed secondary phases (after heating at 1300°C) were $LaSrGa_3O_7$, $La_4Ga_2O_9$, and $LaSrGaO_4$. All of the final precipitates corresponding to the pH versus time traces given in Fig. 1 yielded single-phase LSGZ ceramics after calcination.

Simultaneous TG/DTA traces for a representative precipitate powder (for the samples of $U/C = 30$ and no urease), which had been dried at 90°C, are shown in Fig. 2. Samples showed a total weight loss of about 33%, on heating to 1200°C, which took

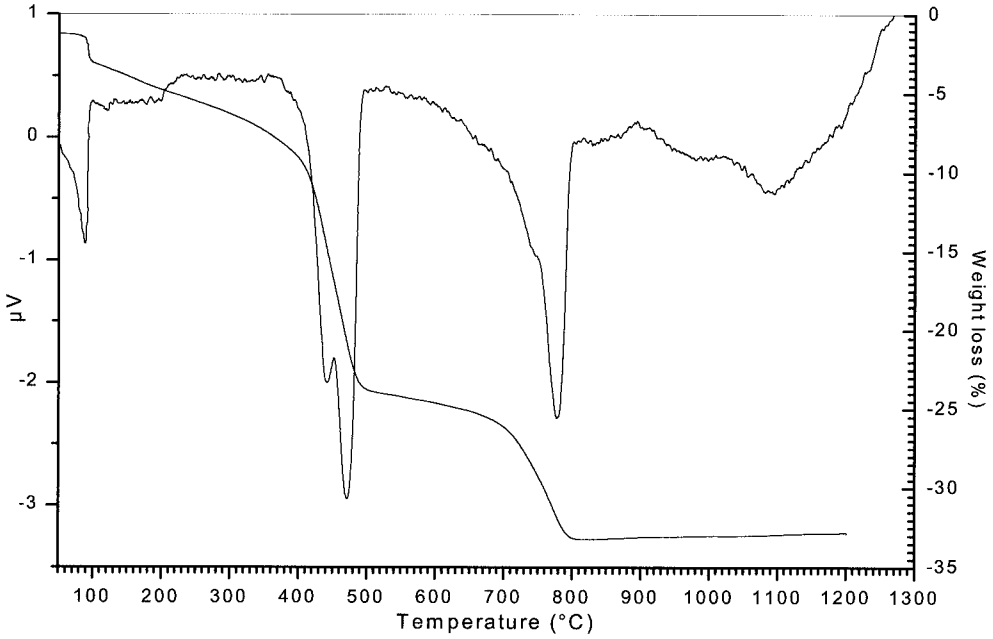

Fig. 2. TG/DTA traces of the LSGZ precursors (5°C/min, air).

place in three steps. A TG trace, which exhibits such distinct steps, is typical for basic hydroxycarbonate powders precipitated in the presence of decomposing urea in aqueous solutions.[43] The first two steps corresponded to a total weight loss of ~23%, while the third amounted to a weight loss of ~10%.

The first endotherm (at 95–100°C) of the DTA trace corresponds to the removal of surface adsorbed H_2O from the precursors. The second (~440°C) and the third (~760°C) endotherms possibly correspond to the removal of hydroxide and carbonate ions, respectively. Therefore, the following reaction may describe the overall conversion of the precursors to the LSGZ ceramic on calcination in air at a temperature >1000°C:

$$(La_{0.8}Sr_{0.2}Ga_{0.8}Zn_{0.2})(OH(CO_3))_{1.867}\cdot H_2O \rightarrow$$
$$La_{0.8}Sr_{0.2}Ga_{0.8}Zn_{0.2}O_{2.8} + 1.934H_2O(g) + 1.867CO_2(g)$$

The total weight loss in the above reaction would reach ~34%, and the same figure obtained from the experimental TG data (i.e., ~33%) would thus be in accord with the above reaction. The EDS analyses performed on these precursor powders (immediately after 90°C drying) gave the following weight percentages for the elements: 32.2 La, 5.15 Sr, 16.21 Ga, and 3.88 Zn. These values were also found to be in close agreement with the proposed hydroxycarbonate formula for the precursors.

The sequence of phase evolution in LSGZ precursor samples was given by the XRD spectra (as a function of increasing calcination temperature) of Fig. 3. Precursor powders, following the 90°C drying step, were found to be crystalline, with an orthorhombic pattern quite similar to those of a previously reported experimental XRD data for $LaAl(OH(CO_3))_2$ precursors,[43] which were also synthesized from aqueous solutions in the presence of decomposing urea. This pattern also resembles that of the mineral ancylite (i.e., $(Ce)(Sr,Ca)(La,Ce)(OH)(CO_3)_2\cdot H_2O$), which was identified by ICDD PDF 29-0384. The powder XRD pattern of this new phase (orthorhombic, space group *Pbnm* (62), with the refined lattice parameters of $a = 8.5932(6)$ Å, $b = 7.4085(5)$ Å, $c = 5.0498(5)$ Å, and $V = 321.48(3)$ Å^3, where the estimated standard deviations in the last significant figure are given in parentheses), with the tentative formula $(La_{0.8}Sr_{0.2}Ga_{0.8}Zn_{0.2})(OH(CO_3))_{1.867}\cdot H_2O$, is given in Table I. Precursors calcined for 6 h at 350°C still had the same diffraction pattern. However, this crystalline phase of the dried precursors disappeared completely on heating to ~500°C.

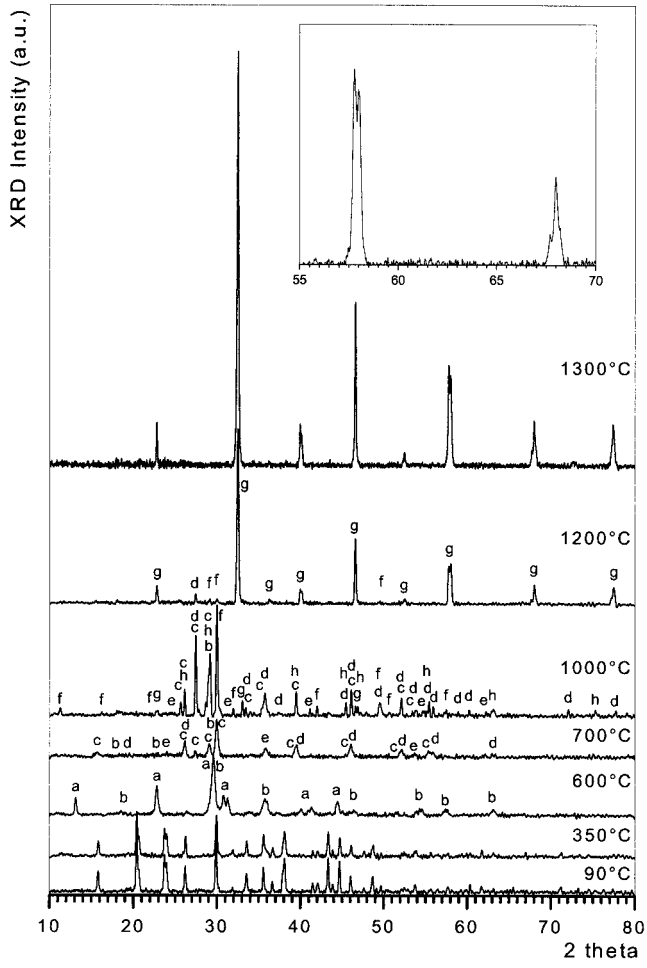

Fig. 3. XRD traces showing the phase evolution in LSGZ precursors. Phases: (a) $La_2(OH(CO_3))_2\cdot H_2O$, (b) $LaSr_2Ga_{11}O_{20}$, (c) LaOOH and $La(OH)_3$ interchangeably, (d) La_2O_3, (e) Ga_2O_3, (f) $SrLaGa_3O_7$, (g) $LaGaO_3$, and (h) La_4SrO_7.

Table I. Powder XRD Pattern of $(La_{0.8}Sr_{0.2}Ga_{0.8}Zn_{0.2})(OH(CO_3))_{1.867}\cdot H_2O$

hkl	d_{calc}	d_{obs}	I/I_0
110	5.6111	5.612	100
101	4.3537	4.354	47
200	4.2966	4.298	66
011	4.1727	4.171	13
111	3.7535	3.755	43
210	3.7168	3.716	94
120	3.4016	3.4014	89
211	2.9933	2.9932	74
021	2.9868	2.9869	70
220	2.8055	2.8051	16
310	2.6717	2.6714	58
002	2.5249	2.5250	19
221	2.4525	2.4521	16
130	2.3734	2.3736	48
311	2.3615	2.3619	44
320	2.2660	2.2656	5
400	2.1483	2.1484	17
131	2.1480	2.1479	20
230	2.1410	2.1414	16
212	2.0886	2.0889	19
022	2.0863	2.0867	18
410	2.0633	2.0631	19
122	2.0274	2.0273	14
231	1.9712	1.9710	20
411	1.9100	1.9101	8
222	1.8768	1.8766	34
040	1.8521	1.8523	8

Table II. Powder XRD Pattern of $La_{0.8}Sr_{0.2}Ga_{0.8}Zn_{0.2}O_{2.80}$

hkl	d_{calc}	d_{obs}	I/I_0
200	3.9115	3.9137	9
011	3.9041	3.9063	12
111	3.4933	3.4932	3
211	2.7632	2.7641	100
002	2.7557	2.7566	46
300	2.6077	2.6081	3
220	2.2581	2.2585	11
202	2.2528	2.2532	9
221	2.0896	2.0899	2
400	1.9558	1.9560	29
022	1.9521	1.9523	41
302	1.8941	1.8942	2
312	1.7919	1.7921	1
411	1.7486	1.7488	3
222	1.7466	1.7468	4
131	1.7063	1.7064	1
231	1.5962	1.5963	25
213	1.5925	1.5925	21
331	1.4522	1.4522	2
422	1.3816	1.3816	5
004	1.3778	1.3778	12
104	1.3569	1.3570	1
413	1.3014	1.3014	2
133	1.2837	1.2836	1
214	1.2651	1.2651	1
611	1.2367	1.2366	6
233	1.2348	1.2347	10

The precursor powders transformed into single-phase LSGZ after single-step calcination (as a loose powder) at temperatures above 1200°C. The phases observed at the intermediary calcination temperatures can be listed as follows (as they appear in the caption of Fig. 3): (a) $La_2(OH(CO_3))_2\cdot H_2O$ (ICDD PDF 46-0368), (b) $LaSr_2Ga_{11}O_{20}$ (45-0646), (c) LaOOH (13-0436) and $La(OH)_3$ (36-1481), interchangeably, (d) La_2O_3 (5-0602), (e) Ga_2O_3 (6-0503), (f) $SrLaGa_3O_7$ (45-0637), (g) $LaGaO_3$ (81-2302), and (h) La_4SrO_7 (22-1430). It should be remembered that since the ICDD PDF database does not yet contain entries for the precursor phases having the nominal LSGZ composition, at this stage we could only use the similar diffraction patterns of various lanthanides (such as phases denoted by (a) and (c)) in indexing our experimental phases. Therefore, the phase assignments given here should not be regarded as absolute, especially for XRD traces up to 1000°C.

As compared with the route of sol–gel synthesis used for the production of LSGM ($La_{0.8}Sr_{0.2}Ga_{0.83}Mg_{0.17}O_{2.815}$) powders, by Huang *et al.*,[30,31] the procedure described in the current work eliminated the need for discrete NH_4OH additions for pH control in the starting solutions, and also eliminated the need for aging of gels at room temperature for 3 days.[31] However, it was also reported[31] that the phase evolution in the sol–gel precursors, as a function of increasing calcination temperature, first went through a stage of multiphase intermediary products at low temperatures, and then the pellets prepared from the sol–gel precursors were converted to single-phase LSGM ceramics only after heating at 1400°C. It has to be noted that the powders of the present study do not even need to be pelletized to form the LSGZ phase at 1300°C.

The crystal structure of the LSGZ samples of this study were found to be "noncubic," in contrast to many reports[3–5,12,30,31] which claimed perfect cubic symmetry for Sr- and Mg-doped $LaGaO_3$ ceramics, and this finding about the crystal structure of LSGZ is in agreement with a recent neutron diffraction study (on LSGM powders) by Slater *et al.*[52] It is known that undoped $LaGaO_3$ adopts an orthorhombic structure (either *Pnma* or *Pbnm*)[53] at room temperature, and in lightly doped (with Sr and Mg) lanthanum gallate the symmetry still remains as orthorhombic.[54] Slater *et al.* reported[52] the observation of either a pseudo-orthorhombic or monoclinic (*I*2/*a*) symmetry for the $La_{0.9}Sr_{0.1}Ga_{0.8}Mg_{0.2}O_{2.85}$ samples, while Skowron *et al.*[54] mentioned the obvious presence of a symmetry lower than cubic in $La_{0.8}Sr_{0.2}Ga_{0.85}Mg_{0.15}O_{2.825}$ ceramics. However, Skowron *et al.* stated that their low-resolution neutron diffraction data did not indicate any significant splitting in the perovskite peaks, although the same data showed the presence of some unindexed (in terms of cubic symmetry) peaks of low intensity.

On the other hand, the inset in Fig. 3 clearly shows the characteristic splitting (55° to 70° 2θ) in the XRD peaks of our $La_{0.8}Sr_{0.2}Ga_{0.8}Zn_{0.2}O_{2.8}$ samples. LSGZ samples of this study were found to have an orthorhombic unit cell with lattice parameters of $a = 7.8231(5)$ Å, $b = 5.5310(5)$ Å, $c = 5.5115(4)$, and $V = 238.48(2)$ Å^3. The space group was *Pnma* (62). A tentative XRD pattern for this new phase has been given in Table II. Rietveld analyses[55,56] were performed (by using the atom positions given by Marti *et al.*[53] for $LaGaO_3$) on the raw XRD data of the LSGZ powders calcined at 1300°C to generate the calculated XRD patterns. It was thus found that those small peaks which Skowron *et al.*[54] recently had a difficulty in indexing under the assumed cubic symmetry were actually the low-intensity peaks of such an orthorhombic structure. A tentative crystal structure drawing of the LSGZ phase is shown in Fig. 4, and the atomic coordinates[53] of this structure are given in Table III. Sr^{2+} and Zn^{2+} ions are substituting for the La^{3+} and Ga^{3+} sites, respectively. Although far from being identical, the structure of LSGZ resembles that of $YFeO_3$ to a certain extent.[57]

FTIR plots (as a function of calcination temperature) of the LSGZ samples are given in Fig. 5. The broad band at 3500–2500 cm^{-1} is due to O–H stretching. Atmospheric CO_2 adsorbed on a metal cation is indicated by the band at 2342 cm^{-1} (for 600°C sample). The existence of a carbonyl bond (C=O stretching vibration) is indicated by the bands in the range of 1800–1730 cm^{-1}. The OH deformation band is seen at 1625 cm^{-1}. The structural CO_3^{2-} is observed by the broad band at 1520–1330 cm^{-1}, also at 1074–1028, 858–805, and 730–696 cm^{-1}. Splitting of the CO_3^{2-} bands is commonly observed[58] in basic carbonates, and such splitting is clearly observed in our data. After calcination at 1300°C, IR bands attributed to anion vibrations disappeared in the LSGZ samples.

The results of carbon analyses were found to be as follows: 6.01, 4.15, 2.34, 0.085, and 0.020 wt% for the 90°, 350°, 600°,

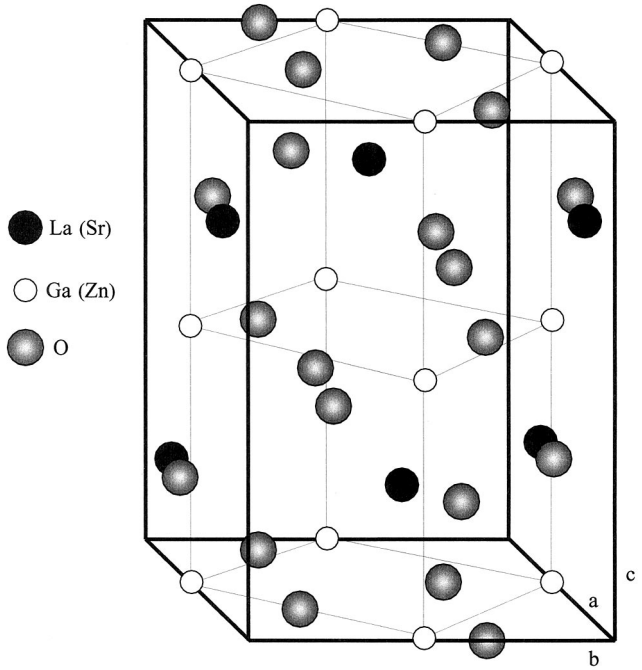

Fig. 4. Orthorhombic unit cell for LSGZ.

1000°, and 1300°C samples, respectively. If one considers that the theoretical carbon content of the assumed precursor formula of $(La_{0.8}Sr_{0.2}Ga_{0.8}Zn_{0.2})(OH(CO_3))_{1.867}{\cdot}H_2O$ is 6.2%, the experimentally determined level (i.e., 6.01%) of carbon in the 90°C-dried sample may be regarded as further confirmation of that stoichiometry. FTIR is a sensitive technique which is able to detect the presence of CO_3^{2-} ions even at a level of 850 ppm (i.e., 1000°C sample). Furthermore, the EDS analyses performed on the 1300°C-calcined powder samples yielded the following mole ratios: La/Sr = 3.98, La/Ga = 0.98, and Ga/Zn = 4.01. These figures experimentally confirmed the theoretical mole ratios of the elements expected to be present in the final, calcined samples, and they also showed that it is possible to replace Mg^{2+} (i.e., LSGM) by Zn^{2+} (i.e., LSGZ). Chemical precipitation in the presence of decomposing urea is, therefore, shown to be able to yield LSGZ ceramics of high elemental uniformity and phase purity.

The powder morphology of LSGZ powders, as a function of calcination temperature, is given by the SEM pictures of Fig. 6. These pictures were taken directly on noncompacted powder samples, following their ultrasonic dispersion in 2-propanol suspensions (20 mg powder in 2 mL of 2-propanol) for a couple of minutes, and drying on the SEM sample holders. The orthorhombic hydroxycarbonate precursor powders which were dried at 90°C and calcined at 350°C (Figs. 6(a) and 6(b)) both had almost the same morphology. The platelike, bigger particles in these micrographs were found (by EDS analyses) to be slightly richer in La and Ga (equimolar), as compared with the smaller, more or less round particles. This means that there have been two different nucleation events taking place in the synthesis beakers, i.e., one for the platelike, and the other for the round, small particles. For this

Table III. Atom Positions for the $La_{0.8}Sr_{0.2}Ga_{0.8}Zn_{0.2}O_{2.80}$ Structure

Ion	*x*	*y*	*z*
La^{3+}	−0.0021	−0.2160	0.25
Sr^{2+}	−0.0021	−0.2160	0.25
Ga^{3+}	0.5	0	0
Zn^{2+}	0.5	0	0
O(1)	0.0709	0.5056	0.25
O(2)	0.7724	0.2273	0.0347

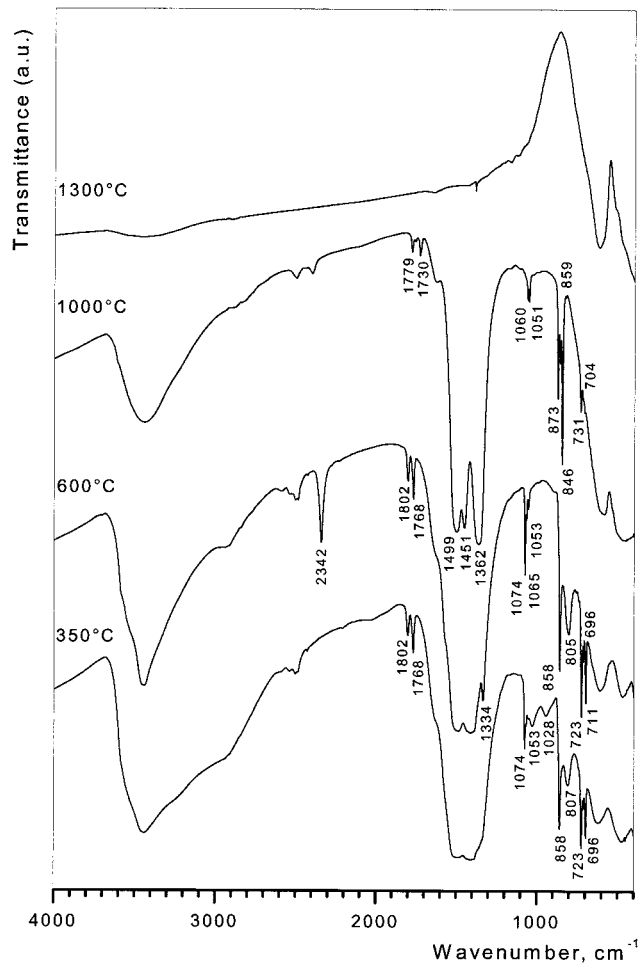

Fig. 5. FTIR spectra of LSGZ powders as a function of calcination temperature.

reason, the process used in this study cannot be called homogeneous precipitation. However, with increasing calcination temperatures (500°, 700°, and 1000°C, i.e., Figs. 6(c), (d), and (e), respectively) these larger particles disappeared, and after calcination at 1000°C (for 6 h), the powder body consisted of round particles with an average diameter of 0.25 μm. These particles of Fig. 6(e) show a significant degree of necking and bonding after calcination at 1000°C. Following calcination at 1300°C, the noncompacted powder body consisted of dense, 20 to 30 μm chunks whose typical surfaces are depicted by the micrograph of Fig. 6(f). The morphologic evolution of the loose LSGZ powder bodies during calcination in alumina boats indicated that such powders are easy to sinter into a dense ceramic with a single, orthorhombic perovskite phase. As indicated in a quite recent study by Sebastian *et al.*,[28] Sr- and Zn-doped $LaGaO_3$ ceramics would exhibit almost pure ionic conductivity, in contrast to doping with other transition-metal elements, like Mn, Co, Ni, or Cu. Measurement of the conductivity of the chemically synthesized powders of the present work will be one of the forthcoming tasks of our group.

IV. Conclusions

A chemical precipitation and powder processing route, which employs the hydrolysis of acidic cations via urea decomposition catalyzed by the enzyme urease, followed by calcination, has been developed for the preparation of powders with a novel composition of $La_{0.8}Sr_{0.2}Ga_{0.8}Zn_{0.2}O_{2.8}$ (i.e., LSGZ). Precursor powders of the precipitation process were shown to have the stoichiometry of

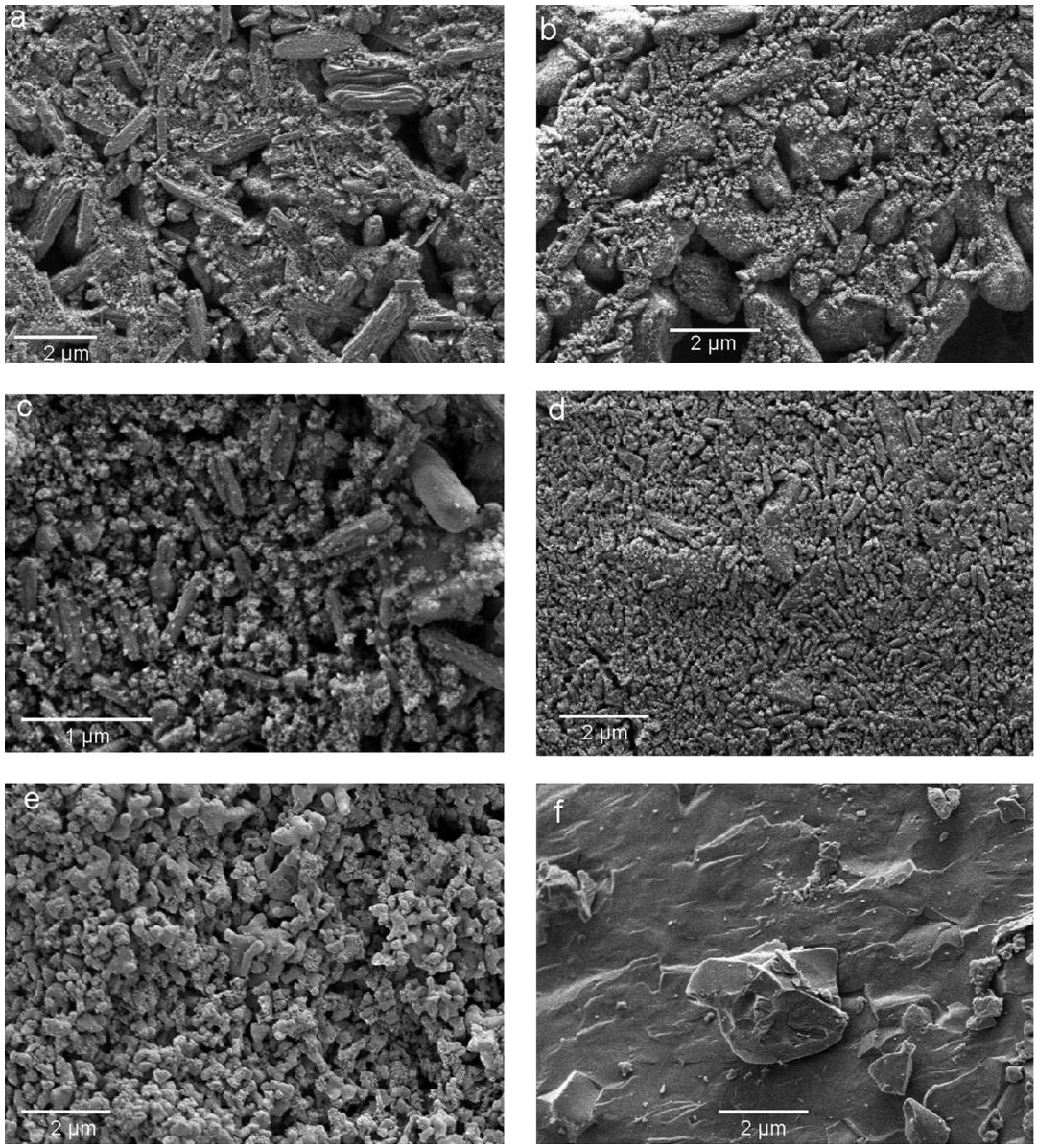

Fig. 6. SEM micrographs of LSGZ powders: (a) 90°, (b) 350°, (c) 500°, (d) 700°, (e) 1000°, (f) 1300°C (6 h, air atmosphere, loose powder calcination).

$(La_{0.8}Sr_{0.2}Ga_{0.8}Zn_{0.2})(OH(CO_3))_{1.867}\cdot H_2O$. A tentative XRD pattern has been presented for these precursors. Hydroxycarbonate precursors were found to transform into single-phase LSGZ after calcination at about 1300°C in an air atmosphere, for 6 h, as a loose powder in alumina boats. An experimental XRD pattern was also created for the $La_{0.8}Sr_{0.2}Ga_{0.8}Zn_{0.2}O_{2.8}$ powders. The high degree of densification achieved even in noncompacted precursors, after calcination at 1300°C, is regarded as promising for further processing and use of such powders in solid oxide fuel cell technology.

Acknowledgments

One of the authors, Dr. A. C. Taş, gratefully acknowledges the Max-Planck-Institute fuer Metallforschung, Stuttgart, for the award of a Visiting Professorship, extending over the term of February 1999 to February 2001. The authors also express their gratitude to M. Thomas (XRD), H. Labitzke (SEM), H. Kummer (TG/DTA), W. Konig (FT-IR), F. Predel (SEM/EDS), and S. Hammoud (C & N analyses) for their generous help with sample characterization.

References

[1]J. P. P. Huijsmans, F. P. F. van Berkel, and G. M. Christie, "Intermediate Temperature SOFC—A Promise for the 21st Century," *J. Power Sources*, **71**, 107–10 (1998).

[2]T. Ishihara, H. Matsuda, and Y. Takita, "Doped $LaGaO_3$ Perovskite Type Oxide as a New Oxide Ionic Conductor," *J. Am. Chem. Soc.*, **116**, 3801–803 (1994).

[3]M. Feng and J. B. Goodenough, "A Superior Oxide-Ion Electrolyte," *Eur. J. Solid. State Inorg. Chem.*, **T31**, 663–72 (1994).

[4]K. Q. Huang, M. Feng, J. B. Goodenough, and C. Milliken, "Electrode Performance Test on Single Ceramic Fuel Cells Using as Electrolyte Sr- and Mg-Doped $LaGaO_3$," *J. Electrochem. Soc.*, **144**, 3620–24 (1997).

[5]K. Q. Huang and J. B. Goodenough, "A Solid Oxide Fuel Cell Based on Sr- and Mg-Doped $LaGaO_3$ Electrolyte: The Role of a Rare-Earth Oxide Buffer," *J. Alloys Compd.*, **303**, 454–464 (2000).

[6]R. Maric, S. Ohara, T. Fukui, H. Yoshida, M. Nishimura, T. Inagaki, and K. Miura, "Solid Oxide Fuel Cells with Doped Lanthanum Gallate Electrolyte and $LaSrCoO_3$ Cathode, and Ni-Samaria-Doped Ceria Cermet Anode," *J. Electrochem. Soc.*, **146**, 2006–10 (1999).

[7]J. Drennan, V. Zelizko, D. Hay, F. T. Ciacchi, S. Rajendran, and S. P. S. Badwall, "Characterization, Conductivity and Mechanical Properties of the Oxygen-Ion Conductor $La_{0.9}Sr_{0.1}Ga_{0.8}Mg_{0.2}O_{3-x}$," *J. Mater. Chem.*, **7**, 79–83 (1997).

[8]N. M. Sammes, F. M. Keppeler, H. Nafe, and F. Aldinger, "Mechanical Properties of Solid-State-Synthesized Strontium- and Magnesium-Doped Lanthanum Gallate," *J. Am. Ceram. Soc.*, **81**, 3104–108 (1998).

[9]S. Baskaran, C. A. Lewinsohn, Y.-S. Chou, M. Qian, J. W. Stevenson, and T. R. Armstrong, "Mechanical Properties of Alkaline-Earth-Doped Lanthanum Gallate," *J. Mater. Sci.*, **34**, 3913–22 (1999).

[10]J. Wolfenstine, "Rate-Controlling Species for Creep of the Solid State Electrolyte: Doped Lanthanum Gallate," *Solid State Ionics*, **126**, 293–98 (1999).

[11]J. Wolfenstine, P. Huang, and A. Petric, "High-Temperature Mechanical Behavior of the Solid-State Electrolyte: $La_{0.8}Sr_{0.2}Ga_{0.85}Mg_{0.15}O_{2.825}$," *J. Electrochem. Soc.*, **147**, 1668–70 (2000).

[12]P. Huang and A. Petric, "Superior Oxygen Ion Conductivity of Lanthanum Gallate Doped with Strontium and Magnesium," *J. Electrochem. Soc.*, **143**, 1644–48 (1996).

[13]K. Q. Huang, R. S. Tichy, and J. B. Goodenough, "Superior Perovskite Oxide-Ion Conductor; Strontium- and Magnesium-Doped $LaGaO_3$: I, Phase Relationships and Electrical Properties," *J. Am. Ceram. Soc.*, **81**, 2565–75 (1998).

[14]J. W. Stevenson, T. R. Armstrong, D. E. McCready, L. R. Pederson, and W. J. Weber, "Processing and Electrical Properties of Alkaline-Earth-Doped Lanthanum Gallate," *J. Electrochem. Soc.*, **144**, 3613–20 (1997).

[15]J. W. Stevenson, T. R. Armstrong, L. R. Pederson, J. Li, C. A. Lewinsohn, and S. Baskaran, "Effect of A-site Cation Nonstoichiometry on the Properties of Doped Lanthanum Gallate," *Solid State Ionics*, **115**, 571–83 (1998).

[16]J. J. Kingsley and K. C. Patil, "A Novel Combustion Process for the Synthesis of Fine Particle α-Alumina and Related Oxide Materials," *Mater. Lett.*, **6**, 427–32 (1988).

[17]L. A. Chick, L. R. Pederson, G. D. Maupin, J. L. Bates, L. E. Thomas, and G. J. Exarhos, "Glycine-Nitrate Combustion Synthesis of Oxide Ceramic Powders," *Mater. Lett.*, **10**, 6–12 (1990).

[18]T. Mathews, J. R. Sellar, B. C. Muddle, and P. Manoravi, "Pulsed Laser Deposition of Doped Lanthanum Gallate and *In Situ* Analysis by Mass Spectrometry of the Laser Ablation Plume," *Chem. Mater.*, **12**, 917–22 (2000).

[19]E. Djurado and M. Labeau, "Second Phases in Doped Lanthanum Gallate Perovskites," *J. Eur. Ceram. Soc.*, **18**, 1397–404 (1998).

[20]R. Maric, T. Fukui, S. Ohara, H. Yoshida, M. Nishimura, T. Inagaki, and K. Miura, "Powder Prepared by Spray Pyrolysis as an Electrode Material for Solid Oxide Fuel Cells," *J. Mater. Sci.*, **35**, 1397–404 (2000).

[21]K. Q. Huang, M. Schroeder, and J. B. Goodenough, "Oxygen Permeation through Composite Oxide-Ion and Electronic Conductors," *Electrochem. Solid State Lett.*, **2**, 375–78 (1999).

[22]T. Ishihara, T. Akbay, H. Furutani, and Y. Takita, "Improved Oxide Ion Conductivity of Co-Doped $La_{0.8}Sr_{0.2}Ga_{0.8}Mg_{0.2}O_3$ Perovskite Type Oxide," *Solid State Ionics*, **115**, 585–91 (1998).

[23]T. Ishihara, T. Shibayama, M. Honda, H. Nishiguchi, and Y. Takita, "Solid Oxide Fuel Cell Using Co-Doped La(Sr)Ga(Mg)O_3 Perovskite Oxide with Notably High Power Density at Intermediate Temperature," *Chem. Commun.*, **13**, 1227–28 (1999).

[24]T. Ishihara, H. Furutani, M. Honda, T. Yamada, T. Shibayama, T. Akbay, N. Sakai, H. Yokokawa, and Y. Takita, "Improved Oxide Ion Conductivity in $La_{0.8}Sr_{0.2}Ga_{0.8}Mg_{0.2}O_3$ by Doping Co," *Chem. Mater.*, **11**, 2081–88 (1999).

[25]N. Trofimenko and H. Ullmann, "Co-Doped LSGM: Composition–Structure–Conductivity Relations," *Solid State Ionics*, **124**, 263–70 (1999).

[26]F. L. Chen and M. L. Liu, "Study of Transition Metal Oxide Doped $LaGaO_3$ as Electrode Materials for LSGM-Based Solid Oxide Fuel Cells," *J. Solid State Electr.*, **3**, 7–14 (1998).

[27]N. Trofimenko and H. Ullmann, "Transition Metal Doped Lanthanum Gallates," *Solid State Ionics*, **118**, 215–27 (1999).

[28]L. Sebastian, A. K. Shukla, and J. Gopalakrishnan, "$La_{0.9}Sr_{0.1}Ga_{0.8}M_{0.2}O_{3-\delta}$ (M = Mn, Co, Ni, Cu, or Zn): Transition Metal-Substituted Derivatives of Lanthanum–Strontium–Gallium–Magnesium (LSGM) Perovskite Oxide Ion Conductor," *Bull. Mater. Sci.*, **23**, 169–73 (2000).

[29]T. Ishihara, T. Shibayama, M. Honda, H. Nishiguchi, and Y. Takita, "Intermediate Temperature Solid Oxide Fuel Cells Using $LaGaO_3$ Electrolyte II. Improvement of Oxide Ion Conductivity and Power Density by Doping Fe for Ga Site of $LaGaO_3$," *J. Electrochem. Soc.*, **147**, 1332–37 (2000).

[30]K. Q. Huang, M. Feng, and J. B. Goodenough, "Sol–Gel Synthesis of a New Oxide-Ion Conductor Sr- and Mg-Doped $LaGaO_3$ Perovskite," *J. Am. Ceram. Soc.*, **79**, 1100–104 (1996).

[31]K. Q. Huang and J. B. Goodenough, "Wet Chemical Synthesis of Sr- and Mg-Doped $LaGaO_3$, A Perovskite-Type Oxide-Ion Conductor," *J. Solid State Chem.*, **136**, 274–83 (1998).

[32]M. Pechini, "Method of Preparing Lead and Alkaline Earth Titanates and Niobates and Coating Method Using the Same to Form a Capacitor," U.S. Pat. No. 3 330 697, July 11, 1967.

[33]N. G. Eror and H. U. Anderson, "Polymeric Precursor Synthesis of Ceramic Materials," *Mater. Res. Soc. Symp. Proc.*, **73**, 571–77 (1986).

[34]P. A. Lessing, "Mixed-Cation Oxide Powders via Polymeric Precursors," *Am. Ceram. Soc. Bull.*, **68**, 1002–1007 (1989).

[35]A. C. Tas, P. J. Majewski, and F. Aldinger, "Chemical Preparation of Pure and Strontium- and/or Magnesium-Doped Lanthanum Gallate Powders," *J. Am. Ceram. Soc.*, **83**, 2954–60 (2000).

[36]E. Matijevic, "Monodispersed Colloids—Art and Science," *Langmuir*, **2**, 12–20 (1986).

[37]E. Matijevic, "Preparation and Properties of Uniform Size Colloids," *Chem. Mater.*, **5**, 412–26 (1993).

[38]L. F. Wang, I. Sondi, and E. Matijevic, "Preparation of Uniform Needle-like Aragonite Particles by Homogeneous Precipitation," *J. Colloid Interface Sci.*, **218**, 545–53 (1999).

[39]M. Akinc, N. Jongen, J. Lemaitre, and H. Hofmann, "Synthesis of Nickel Hydroxide Powders by Urea Decomposition," *J. Eur. Ceram. Soc.*, **18**, 1559–64 (1998).

[40]D. J. Sordelet, M. Akinc, M. L. Panchula, Y. Han, and M. H. Han, "Synthesis of Yttrium–Aluminum–Garnet Precursor Powders by Homogeneous Precipitation," *J. Eur. Ceram. Soc.*, **14**, 123–30 (1994).

[41]A. Celikkaya and M. Akinc, "Preparation and Mechanism of Formation of Spherical Submicrometer Zinc Sulfide Powders," *J. Am. Ceram. Soc.*, **73**, 2360–65 (1990).

[42]D. Sordelet and M. Akinc, "Preparation of Yttrium, Lanthanum, Cerium, and Neodymium Basic Carbonate Particles by Homogeneous Precipitation," *Adv. Ceram. Mater.*, **2**, 232–38 (1987).

[43]E. Taspinar and A. C. Tas, "Low-Temperature Chemical Synthesis of Lanthanum Monoaluminate," *J. Am. Ceram. Soc.*, **80**, 133–41 (1997).

[44]L. J. Gauckler, T. Graule, and F. Baader, "Ceramic Forming Using Enzyme Catalyzed Reactions," *Mater. Chem. Phys.*, **61**, 78–102 (1999).

[45]D. E. Appleman and H. T. Evans, "Indexing and Least-Squares Refinement of Powder Diffraction Data," *U.S. Geol. Surv.*, **GD-73-003** (1973).

[46]H. H. Willard and N. K. Tang, "Precipitation of Al Basic Sulfate by Urea," *J. Am. Chem. Soc.*, **59**, 1190–96 (1937).

[47]R. E. Simpson, C. Habeger, A. Rabinovich, and J. H. Adair, "Enzyme-Catalyzed Inorganic Precipitation of Aluminum Basic Sulphate," *J. Am. Ceram. Soc.*, **81**, 1377–79 (1998).

[48]D. Bayraktar and A. C. Tas, "Preparation of Biomimetic HA Precursors at 37°C in Urea- and Enzyme Urease-Containing Synthetic Body Fluids"; pp. 39–52 in Ceramic Transactions, Vol. 110, *Bioceramics: Materials and Applications III*. Edited by L. George, R. P. Rusin, G. Fischman, and V. Janas. American Ceramic Society, Columbus, OH, 2000.

[49]W. H. R. Shaw and J. J. Bordeaux, "The Decomposition of Urea in Aqueous Media," *J. Am. Chem. Soc.*, **77**, 4729–4733 (1955).

[50]B. C. Cornilsen and J. E. Reed, "Homogeneous Precipitation of Basic Aluminum Salts as Precursors for Alumina," *Am. Ceram. Soc. Bull.*, **58**, 1999 (1979).

[51]Z.-P. Xie, Y.-L. Chen, and Y. Huang, "A Novel Casting Forming for Ceramics by Gelatine and Enzyme Catalysis," *J. Eur. Ceram. Soc.*, **20**, 253–57 (2000).

[52]P. R. Slater, J. T. S. Irvine, T. Ishihara, and Y. Takita, "The Structure of the Oxide Ion Conductor $La_{0.9}Sr_{0.1}Ga_{0.8}Mg_{0.2}O_{2.85}$ by Powder Neutron Diffraction," *Solid State Ionics*, **107**, 319–23 (1998).

[53]W. Marti, P. Fischer, F. Altorfer, H. J. Scheel, and M. Tadin, "Crystal Structures and Phase Transitions of Orthorhombic and Rhombohedral $RGaO_3$ (R = La, Pr, Nd) Investigated by Neutron Powder Diffraction," *J. Phys.: Condens. Matter*, **6**, 127–35 (1994).

[54]A. Skowron, P. N. Huang, and A. Petric, "Structural Study of $La_{0.8}Sr_{0.2}Ga_{0.85}Mg_{0.15}O_{2.825}$," *J. Solid State Chem.*, **143**, 202–209 (1999).

[55]H. M. Rietveld, "A Profile Refinement Method for Nuclear and Magnetic Structures," *J. Appl. Crystallogr.*, **2**, 65–71 (1969).

[56]A. Sakthivel and R. A. Young, "Rietveld Analysis of X-ray Powder Diffraction Patterns: Program DBWS-9807, Version: September 1998," School of Physics, Georgia Institute of Technology, Atlanta, GA 30332.

[57]D. du Boulay, E. N. Maslen, and V. A. Streltsov, "A Synchrotron X-ray Study of the Electron Density in $YFeO_3$," *Acta Crystallogr.*, **B51**, 921–929 (1995).

[58]G. Socrates, *Infrared Characteristic Group Frequencies*. Wiley, New York, 1994. □